Eur. Phys. J. C (2026) 86:289
https://doi.org/10.1140/epjc/s10052-026-15502-9

THE EUROPEAN PHYSICAL JOURNAL C

Regular Article - Experimental Physics

Measurement of the cosmic-ray rate over the period 2019–2025 at very high latitude (78.9°N)

M. Abbrescia[1,2], C. Avanzini[3,4], L. Baldini[3,4], R. Baldini Ferroli[5], G. Batignani[3,4,12], M. Battaglieri[6], E. Bossini[4], F. Carnesecchi[5,12], D. Cavazza[10], C. Cicalò[8], L. Cifarelli[10,11,12], F. Coccetti[12], E. Coccia[13], A. Corvaglia[14], A. De Caro[12,15,16], D. De Gruttola[12,15,16], S. De Pasquale[12,15,16], L. Galante[17], M. Garbini[10,12], L. E. Ghezzer[34], I. Gnesi[12,18], F. Gramegna[23], E. Gramstad[32], S. Grazzi[6,19], E. S. Haland[32], D. Hatzifotiadou[9,10], P. La Rocca[20,21,12,a], R. Liotino[2,12], G. Mandaglio[19,21], A. Margotti[10], G. Maron[23], M. N. Mazziotta[2], A. Mulliri[7,8], R. Nania[10,12], F. Noferini[10,12], F. Nozzoli[24,34], F. Ould-Saada[32], F. Palmonari[10,11], M. Panareo[14,25], M. P. Panetta[2], R. Paoletti[4,26], C. Pellegrino[27], L. Perasso[6], O. Pinazza[10,12,9,b], C. Pinto[9], S. Pisano[5,12], K. Piscicchia[5,12], L. Quaglia[33], M. Rasà[12,20,21], F. Riggi[12,20,21], G. Righini[28], C. Ripoli[12,15,16], M. Rizzi[2], B. Sabiu[10,11], G. Sartorelli[10,11], E. Scapparone[10], M. Schioppa[18,29], G. Scioli[10,11], A. Scribano[4,26], M. Selvi[10], A. Shtimermann[27], M. Taiuti[6,30], A. Trifirò[19,21], M. Trimarchi[19,21], C. Vistoli[27], L. Votano[31], M. C. S. Williams[9,22], A. Zichichi[9,10,11,12,22], R. Zuyeuski[9,22]

[1] Dipartimento di Fisica “M. Merlin”, Università e Politecnico di Bari, Via Amendola 173, 70125 Bari, Italy
[2] INFN, Sezione di Bari, Via Orabona 4, 70126 Bari, Italy
[3] Dipartimento di Fisica “E. Fermi”, Università di Pisa, Largo Bruno Pontecorvo 3, 56127 Pisa, Italy
[4] INFN, Sezione di Pisa, Largo Bruno Pontecorvo 3, 56127 Pisa, Italy
[5] INFN, Laboratori Nazionali di Frascati, Via Enrico Fermi 54, 00044 Frascati (RM), Italy
[6] INFN, Sezione di Genova, Via Dodecaneso 33, 16146 Genova, Italy
[7] Dipartimento di Fisica, Università di Cagliari, S.P. Monserrato-Sestu km 0.700, 09042 Monserrato (CA), Italy
[8] INFN, Sezione di Cagliari, S.P. Monserrato-Sestu Km 0.700, 09042 Monserrato (CA), Italy
[9] European Organisation for Nuclear Research (CERN), Esplanade des Particules 1, 1211 Geneva 23, Switzerland
[10] INFN Sezione di Bologna, Viale Carlo Berti Pichat 6/2, 40127 Bologna, Italy
[11] Dipartimento di Fisica e Astronomia “A. Righi”, Università di Bologna, Viale Carlo Berti Pichat 6/2, 40127 Bologna, Italy
[12] Museo Storico della Fisica e Centro Studi e Ricerche “E. Fermi”, Via Panisperna 89a, 00184 Roma, Italy
[13] Gran Sasso Science Institute, Viale Francesco Crispi 7, 67100 L’Aquila, Italy
[14] INFN Sezione di Lecce, Via per Arnesano, 73100 Lecce, Italy
[15] Dipartimento di Fisica “E. R. Caianiello”, Università di Salerno, Via Giovanni Paolo II 132, 84084 Fisciano, Italy
[16] INFN Gruppo Collegato di Salerno, Via Giovanni Paolo II 132, 84084 Fisciano, Italy
[17] Teaching and Language Lab, Politecnico di Torino, Corso Duca degli Abruzzi 24, Torino, Italy
[18] INFN Gruppo Collegato di Cosenza, Via Pietro Bucci, Rende (Cosenza), Italy
[19] Dipartimento di Scienze Matematiche e Informatiche, Scienze Fisiche e Scienze della Terra, Università di Messina, Viale Ferdinando Stagno d’Alcontres 31, 98166 Messina, Italy
[20] Dipartimento di Fisica e Astronomia “E. Majorana”, Università di Catania, Via S. Sofia 64, 95123 Catania, Italy
[21] INFN Sezione di Catania, Via S. Sofia 64, 95123 Catania, Italy
[22] ICSC World Laboratory, Geneva, Switzerland
[23] INFN Laboratori Nazionali di Legnaro, Viale dell’Università 2, 35020 Legnaro, Italy
[24] INFN Trento Institute for Fundamental Physics and Applications, Via Sommarive 14, 38123 Trento, Italy
[25] Dipartimento di Matematica e Fisica “E. De Giorgi”, Università del Salento, Via per Arnesano, 73100 Lecce, Italy
[26] Dipartimento di Scienze Fisiche, della Terra e dell’Ambiente, Università di Siena, Via Roma 56, 53100 Siena, Italy
[27] INFN-CNAF, Viale Carlo Berti Pichat 6/2, 40127 Bologna, Italy
[28] CNR, Istituto di Fisica Applicata “Nello Carrara”, Via Madonna del Piano 10, 50019 Sesto Fiorentino (FI), Italy
[29] Dipartimento di Fisica, Università della Calabria, Via Pietro Bucci, Rende (CS), Italy
[30] Dipartimento di Fisica, Università di Genova, Via Dodecaneso 33, 16146 Genova, Italy
[31] INFN Laboratori Nazionali del Gran Sasso, Via G. Acitelli 22, 67100 Assergi (AQ), Italy
[32] Physics Department, Oslo University, P.O.Box 1048, 0316 Oslo, Norway
[33] INFN Sezione di Torino, Via Pietro Giuria 1, 10125 Torino, Italy
[34] Dipartimento di Fisica Università di Trento, via Sommarive 14, 38123 Trento, Italy

Received: 10 October 2025 / Accepted: 25 February 2026

Published online: 20 March 2026

Abstract Since 2019, the Extreme Energy Events (EEE) Project has installed three muon detection stations at the Svalbard Islands (78.9°N latitude), employing scintillator-based detectors. This initiative represents the first systematic effort to monitor cosmic-muons rates at high geomagnetic latitudes beyond the Arctic Circle, with the objective of improving our understanding of cosmic-ray propagation and modulation in polar regions. The present study analyses temporal variations in the muon detection rates over a six-year period (2019–2025), including the study of periodic modulations and underlying trends in the observed rates.

1 Introduction

The Extreme Energy Events (EEE) Project combines in a unique way an experiment for the measurements of cosmic-ray rates over a large area, with a dedicated outreach programme [1]. It is supported by two Italian research institutes within the Ministry of University and Research, namely the "Enrico Fermi" Historical Museum of Physics, and Research and Study Centre (CREF) and the National Institute for Nuclear Physics (INFN). The experiment employs two types of detectors: more than 50 measuring stations equipped with Multigap Resistive Plate Chambers (MRPCs), distributed across various high schools and research laboratories in Italy [2], and four stations equipped with scintillator detectors (referred to as POLA-R detectors), three of which are located at the Svalbard Islands (78.9°N) [3,4]. These POLA-R stations represent the only permanent installations dedicated to the measurement of cosmic muons at high latitudes, beyond the Arctic Circle.[1]

Both types of detectors (MRPCs and POLA-Rs) have been built, operated, and monitored not only by researchers from the aforementioned institutes but also by high-school students. Moreover, these students actively participate in monthly collaboration meetings, where they are encouraged to present simple analyses, in line with the project's original objectives. EEE has been running for over 20 years [5].

In this paper, the cosmic muon rates measured with the POLA-R stations located at the Svalbard Islands are reported. The measurements cover a period of six years, between 2019 and 2025. After a description of the experimental setup, of the track reconstruction and correction procedures, the time series are analysed in terms of pseudo-periodicity and solar-cycle dependence.

[a] e-mail: paola.larocca@ct.infn.it (corresponding author)

[b] e-mail: Ombretta.Pinazza@cern.ch (corresponding author)

[1] The POLA-R stations distinguish the so-called PolarquEEEst (sub)Project within the EEE Project.

2 Experimental setup

2.1 Description of a POLA-R detector

The results reported in this study are based on measurements by three POLA-R detection stations. Each one consists of 8 scintillator tiles (30x20 cm^2) positioned on two planes at a distance of 11 cm. Each tile is readout by two silicon photomultipliers (SiPMs) placed on opposite corners. The two planes are mounted inside a light-tight box. The 16 signals from the SiPMs are amplified and discriminated and sent to a trigger and readout board equipped with time-to-digital converters (TDCs) with leading and trailing recording [6]. The event trigger requires at least three SiPM signals to be within a 10 ns time-coincidence window, with at least one on a different plane. Data are collected alongside a set of parameters essential for the analysis: GPS timestamp, atmospheric pressure, temperature outside and inside the cover box and electronics. A more detailed description of the apparatus can be found in [3].

One of these stations provided measurements beyond the Arctic Circle up to 82°N, during a scientific expedition on board of a sailing boat, while the other two stations were placed inside schools in Italy and Norway and were used as reference [3]. The same station used on the boat was also used for a campaign of measurements by car "on the road" with the purpose of investigating the rate as a function of the latitude in the interval 32°- 82°N [7].

2.2 Installation setup at Ny-Ålesund

Since June 2019, three POLA-R stations are positioned in the permanent international research site of Ny-Ålesund, located on the north western coast of Spitsbergen, the largest island in the Svalbard archipelago (see Fig. 1). All three stations are placed in protected places managed by the Italian National Research Council (CNR), with electricity, minimal heating and internet connection. More specifically, POLA-1 is hosted inside the Climate Change Tower hutch, POLA-3 in the Dirigibile Italia Arctic Station, and POLA-4 in the Gruvebadet Laboratory. A fourth station, POLA-2, is placed in the EEE laboratory at INFN Bologna and is used as a reference.

Measurements carried out with the three POLA-R detectors have already allowed the publication of an analysis of the Forbush decrease observed during the major geomagnetic storm of May 2024 [4]. Moreover, thanks to the atmospheric pressure sensors with which the detectors are equipped, it was possible to observe the Rayleigh-Lamb waves generated by the 2022 Hunga-Tonga volcanic eruption [8].

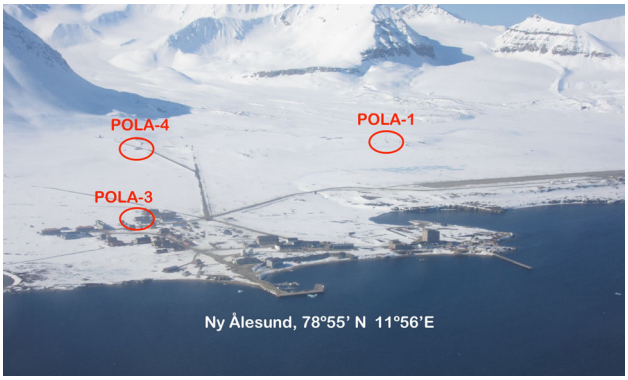

Fig. 1 Aerial photo of the international research site at Ny-Ålesund, Svalbard archipelago. The red circles indicate the exact position of the three POLA-R stations. Photo courtesy: PolarquEEEst Project

3 Reconstruction and corrections of rate time series

3.1 Data taking and reconstruction

Data measured by POLA-Rs are first saved locally, and then synchronised with the remote repository at INFN-CNAF computer centre in Bologna (Italy), where the EEE Project's computing infrastructure has being operational for several years. All events are analysed and collected in bins with a duration of 1 min, together with their GPS tags and environment parameters. During this phase, the quality of individual events is also assessed through a quality flag, tagging cases where the sensor readings are incorrect, or the duration of the integration interval is not as desired.

For the present analysis, cuts excluding low quality events are applied, specifically to exclude cases of wrong pressure readings, or excessive internal temperatures, which would imply bad behaviour of the readout electronics.

3.2 Pseudo-efficiency correction

As previously mentioned, the trigger condition requires signals from at least three out of four SiPMs (two SiPMs per plane), implementing a majority logic. This setup enables the measurement and continuous monitoring of individual SiPM efficiencies over time.

Under the assumption of linear propagation for small corrections to the majority condition, the majority efficiency was calculated and applied, the so-called pseudo-efficiency correction. While this correction represents the best current estimate of the detector's status, it still relies on certain assumptions, and residual uncertainties may affect the measurement.

Given that each plane is composed of four tiles, we analyzed the four possible vertical pair combinations. After applying efficiency corrections, the trigger rates for these pairs are expected to be consistent. To quantify potential systematic effects arising from nonlinearities in the majority-condition efficiency calculation, the corrected rates of the vertical pairs were compared. Any observed deviations were assigned as a systematic uncertainty. When the rate is averaged in a larger time interval its value is calculated as a weighted average, being the weight equal to $1/syst^2$ in order to optimize/minimize systematic uncertainties.

3.3 Rate time series

The muon rate time series are obtained from the accepted events with the correction factor related to the pseudo-efficiencies. No acceptance corrections are applied to the measured values, since in this study only the relative variations with time are reported.

The plot in Fig. 2 shows a sample of rates recorded by the three POLA-R detectors during six months in 2025 with one minute binning (coloured dots), and their 24 h running average (coloured solid line). The gaps are due to malfunc-

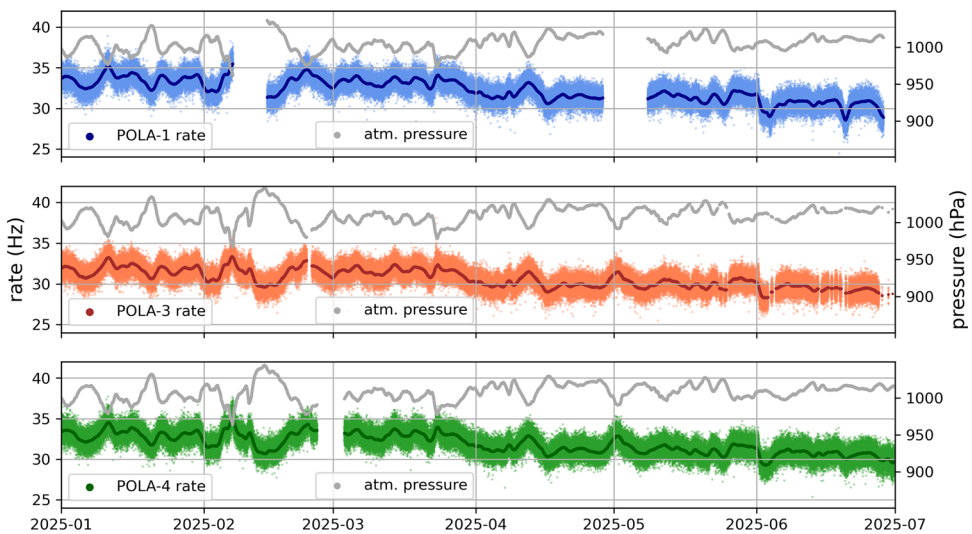

Fig. 2 POLA-R rates during the first semester of 2025. The one minute binning (coloured dots) and their 24 h running average (coloured solid line) are shown. The atmospheric pressure is also reported (solid grey line)

tioning of the detectors or power interruptions in the CNR research base at Ny-Ålesund, that were sometimes difficult to recover, due to the remoteness of the site. The grey curves represent atmospheric pressure at ground level, measured by the POLA-R sensors; even at a first glance, the anti-correlation between rate and pressure is evident. The barometric correction is described in Sect. 3.4.

3.4 Barometric correction

Commonly acknowledged and extensively described in scientific literature [9], the effect of atmospheric pressure on the secondary particle rate measured on the ground is defined as:

$$I_P = I_0\, e^{-0.01\ \beta\ (P-P_0)} \tag{1}$$

where I_P is the muon count rate expected when the atmospheric pressure (hPa) is equal to P, considering an initial count rate I_0, observed when the atmospheric pressure corresponds to a chosen value P_0.

β is the barometric coefficient (%/hPa) representing the magnitude of pressure influence, that can be computed from the simple linear regression between $\Delta I = I - \langle I \rangle$ and $log(\Delta P/\langle P \rangle)$, where $\langle I \rangle$ and $\langle P \rangle$ are the mean rate and the mean pressure [9]. For our studies, the barometric correction coefficient β is evaluated over the whole analysis period, independently for each of the detectors: the data and the fit results are illustrated in Fig. 3.

4 Results and pseudo-periodicity analysis

After reconstruction, analysis selection, pseudo-efficiency and barometric correction, the final rate and differential rate time series are reported in Fig. 4, where the differential rate is expressed as

$$\Delta I(t) = 100 * \frac{I(t) - \langle I \rangle}{\langle I \rangle} \tag{2}$$

with $\langle I \rangle$ being the mean rate evaluated over the entire time interval.

The three detectors present a very good overall stability with a excellent precision on the rate measurements, as shown by the error bars (mainly systematic) in grey.

4.1 Muon rate pseudo-periodicity

The muon rate time series exhibit a clear periodic behavior, with a fairly regular amplitude and a frequency of approximately one year, providing the evidence of a seasonal variation at such a high latitude. However, the production of secondary cosmic rays is not, by its nature, a strictly periodic process since the temporal behavior observed in the data is governed by phenomena that exhibit variable characteristics. Among these are atmospheric temperature variations and, more broadly, changes in the vertical structure and density profile of the Earth's atmosphere, which directly influence secondary particle production and propagation. The superposition and time variability of these atmospheric effects constitute one of the primary physical reasons why the muon flux measured at the Earth's surface displays pseudo-periodic, rather than strictly periodic, behaviour [9].

To quantify the observed time modulation, various mathematical methods can be used. The POLA-R time series are characterized by measurements that are fairly regular in time but contain gaps, due to detector malfunctions, special calibration runs, or simply events rejected due to poor quality. This aspect makes it difficult to use the Fast Fourier Transform (FFT) to detect the periodic component from the data.

For this reason the periodicity analysis was performed with the Least Squares Spectral Analysis (LSSA), consisting in least-squares fitting of selected frequencies of sinusoids. First introduced some time ago, LSSA techniques have since been improved in astronomy to recognise periodic patterns in data sets with irregular observation times. One of the practical implementations of spectral analysis techniques is the Lomb-Scargle periodogram [10].

When applying the periodogram technique to the POLA-R six-year time series, we obtain the results shown in Fig. 5. Note the prominent peak at a pseudo-period of 366–372 days, confirming a dominant annual variation.

Additional excesses at periods of approximately two years and longer indicate the possible presence of other periodic components. However, these cannot yet be resolved using the Lomb-Scargle periodogram, due to the limited six-year span of the available time series. This limitation is particularly relevant for detecting the solar cycle, which has a characteristic period of approximately 11 years, with last minimum that occurred in December 2019 and next maximum expected in the second half of 2025 (whose confirmation is ongoing). Figure 4 clearly reveals a declining trend in the rate over time, consistent with the expected anti-correlation of the muon rate with the evolution of the solar cycle over this interval.

The cosmic-ray rate, averaged over the three POLA-R detectors, is represented in Fig. 6. Overlaid on the data is a double sinusoidal function (red line), obtained through a nonlinear least-squares fit, consisting of a quasi-annual component with a period of 366 days and an amplitude of $(2.89 \pm 0.04)\%$, and a solar-cycle component with a period of 11.16 years. The latter is also shown separately as a dashed blue line.

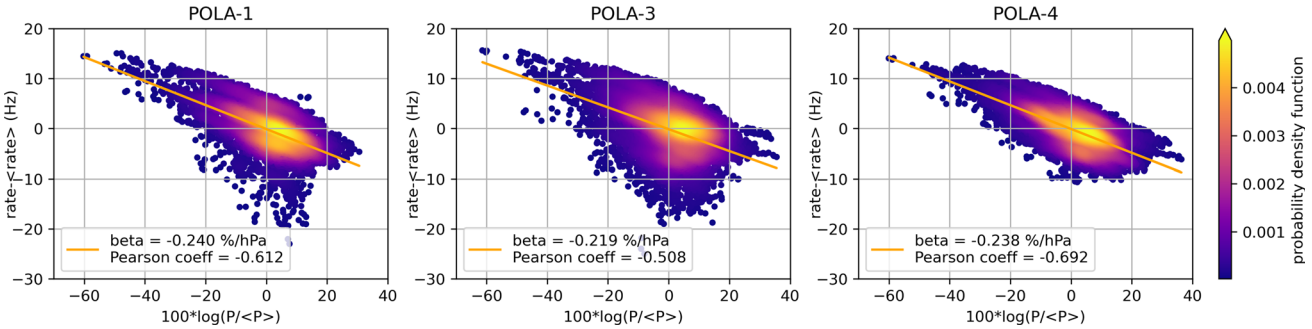

Fig. 3 Barometric correction. The three density plots show the correlation between the uncorrected differential rate and the logarithm of the relative variation of atmospheric pressure for the three POLA-R time series. The colormap represents the probability density function estimated using a Gaussian Kernel Density Estimation (KDE). The superimposed straight line shows the result of the linear fit described in the text, from which the parameter β is derived. The boxes report the β values and the Pearson correlation coefficients

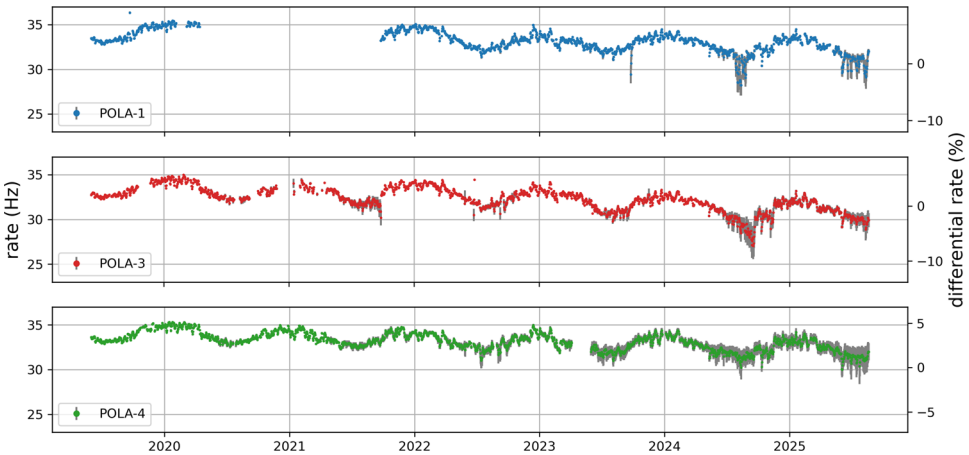

Fig. 4 POLA-R pressure-corrected rates (Hz) and differential rates (%, right axis) resampled with 1-day resolution. The error bars (in grey) represent the combination of statistical errors on the rates, obtained through resampling, and systematic errors, evaluated from the pseudo-efficiency of the single SiPMs

4.2 Comparison with other detectors

The geomagnetic cutoff rigidity strongly depends on latitude, approaching nearly zero near the poles. As a result, a larger fraction of low-energy muons can reach the ground at high latitudes, leading to an increased muon counting rate and a plateau above approximately 60°N [7]. This variation in low-energy muon flux can influence the observed seasonal modulation when comparing data from higher and lower latitudes. Moreover, the ground pressure correction, as described in the literature [9], still leaves a residual modulation related to the atmospheric conditions above the measurement site. Because the atmospheric structure varies with latitude and affects low- and high-energy muons differently, these variations can further modify the seasonal modulation. For all these reasons, a detailed study of the latitude dependence of the seasonal modulation is essential to gain insight into how the ground-level cosmic muon production rate varies both in

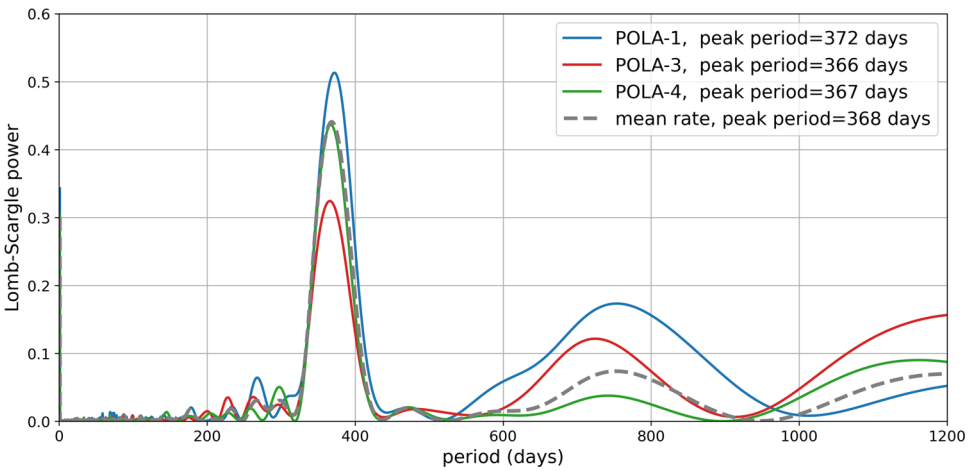

Fig. 5 Lomb-Scargle periodogram for the rate time series of the three POLA-Rs and for the average rate

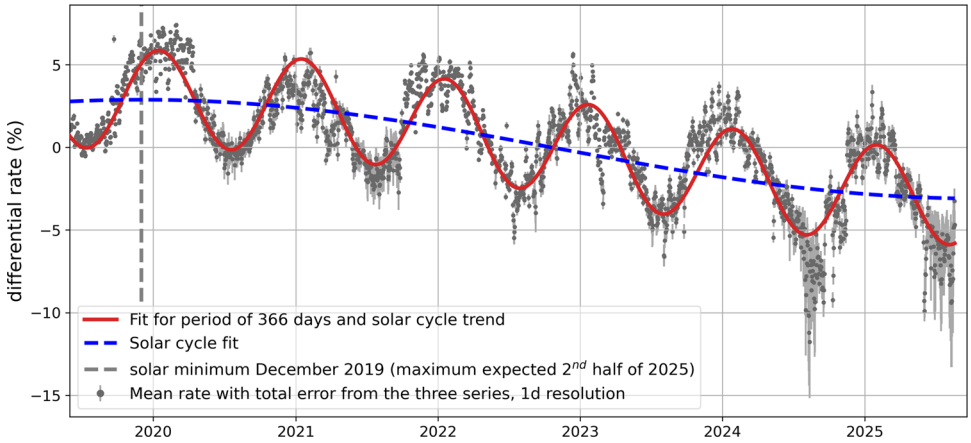

Fig. 6 Average rate of the three POLA-R stations. Uncertainties combine statistical errors, calculated as the mean squared error of the three time series, and systematic errors. The pseudo-annual periodic fit and solar-cycle trend are reported. A reference to the solar-cycle minimum is also shown (grey dashed line)

time and with latitude. Such a study is currently underway to quantify the necessary atmospheric parameter corrections to the present data and to compare them with the results reported in [9]. In the following, only a qualitative overview of a few other experiments is presented.

The present results on annual pseudo-periodicity are qualitatively consistent with the Global Muon Detector Network (GMDN) data reported in [9]. The data shown in Fig. 6 tend to exhibit a higher amplitude compared to those reported for GMDN stations in the Northern Hemisphere (Nagoya, Japan, and Kuwait City, Kuwait), and even more if compared to those in the Southern Hemisphere (São Martinho da Serra, Brazil, and Hobart, Australia) [11].

Vertical data from the YBJ International Cosmic Ray Observatory in Yangbajing, China, also display a clear annual periodicity [12], with an amplitude slightly higher than that observed by POLA-R stations at Ny-Ålesund.

However, all these measurements were conducted at significantly lower latitudes than those considered in this study, and in the case of Yangbajing, at a much higher altitude. Moreover, the methods for acceptance and correction applied vary between studies. For all these reasons, a direct comparison is difficult.

In the Southern Hemisphere, ground-level data from the Syowa SYO_MD_V station at 69°S [13] show a seasonal modulation with an amplitude comparable to that observed in the present analysis. Measurements from the ICE-CUBE collaboration at even higher latitudes (89°S) also exhibit seasonal modulation [14]; however, the detected muon energies are much higher than those considered here and these measurements are more appropriately compared with those from other underground experiments, such as LVD at the INFN Laboratory in Gran Sasso (42°N) in Italy [15].

No annual pseudo-periodicities are instead observed by the neutron stations [16], where the solar-cycle pseudo-periodicity is dominating. In particular, at latitudes similar to those of the present data, this behaviour is observed at ground level in both the Northern Hemisphere (Oulu, 65°N) and the Southern Hemisphere (Syowa Station, 69°S [13]. At even higher latitudes (75°S) and altitudes (3200 m), the CHINSTRAP research project, with its neutron station located at Dome C on the Antarctic Plateau, also reports a similar trend with no evidence of season modulation [16]. However, in [17], integrating a very large number of years, small annual variations less than 1% are reported.

5 Conclusions

Within the EEE Project, three POLA-R scintillator detectors have been taking data for more than 6 years (from 2019 till 2025) at the Svalbard Islands (78.9° N latitude), being the highest latitude permanent measuring stations for cosmic-muon monitoring. The detectors showed a very good stability in operation and consistent results, allowing a very precise rate measurement.

The data provide a clear evidence of seasonal variation, with similar results for all three devices. The main pseudo-periodicity of the variations was analyzed using the Lomb–Scargle periodogram, which revealed a periodic component with a period of 366–372 days. A subsequent analysis, employing a nonlinear least-squares fit to optimize a sinusoidal model, confirmed the presence of an oscillation with a period of 366 days and an amplitude of $(2.89 \pm 0.04)\%$. In addition, the model suggests the presence of a solar-cycle component with a period of 11.16 years. This unprecedented and precise estimate, obtained well beyond the Arctic Circle, provides a valuable benchmark for comparison with other measurements performed in the Antarctic regions or at different latitudes, altitudes, and energy ranges.

Acknowledgements The authors would like to thank the Institute of Polar Sciences of the National Research Council (CNR-ISP) hosting the POLA-R detectors at the CNR facilities in Ny-Ålesund, and the personnel of the Dirigibile Italia Arctic Station for their help in the management and monitoring of the detectors. We would also like to acknowledge GMDN (Global Muon Detector Network), NMDB (Neutron Monitor DataBase) and IHEP (Institute of High Energy Physics, Chinese Academy of Sciences) for providing access to the data.

Funding The Extreme Energy Events (EEE) Project is supported by the "Enrico Fermi" Historical Museum of Physics, and Research and Study Centre (CREF) and the National Institute for Nuclear Physics (INFN), and is funded by the Italian Ministry of University and Research.

Data Availibility Data will be made available on reasonable request. [Author's comment: The datasets analysed during the current study are available from the corresponding author on reasonable request.]

Code Availability Statement This manuscript has no associated code/software. [Author's comment: No code/software is available.]

Funded by SCOAP[3].

References

1. A. Zichichi, Extreme Energy Events - La Scienza nelle Scuole (2017). https://eee.centrofermi.it/images/EEE-PaperAZ/EEE_Paper_AZ-2017.pdf
2. M. Abbrescia et al., Performance of the multigap resistive plate chambers of the extreme energy event experiment. JINST **14**(C05022) (2019) https://doi.org/10.1088/1748-0221/14/05/C05022
3. M. Abbrescia et al., New high precision measurements of the cosmic charged particle rate beyond the arctic circle with the PolarquEEEst experiment. Eur. Phys. J. C **80-665** (2020) https://doi.org/10.1140/epjc/s10052-020-8213-2
4. F. Riggi et al., High latitude observation of the forbush decrease during the May 2024 solar storms with muon and neutron detectors on svalbard. Adv. Space Res. (2025). https://doi.org/10.1016/j.asr.2025.05.023
5. M. Abbrescia et al., Bringing the science to the hearts of young people The Extreme Energy Events project (2004-2024). Submitted to Supplemento al Giornale di Fisica (2024)
6. R. Travaglini et al., A multi-channel trigger and acquisition board for TDC-based readout: application to the cosmic rays detector of the PolarQuEEEst 2018 project. *Proceedings of Topical Workshop on Electronics for Particle Physics — PoS(TWEPP2019)*, 370, 150 (2020). https://doi.org/10.22323/1.370.0150
7. M. Abbrescia et al., Measurement of the cosmic charged particle rate at sea level in the latitude range 35-82 N with the polarqueeest experiment. Eur. Phys. J. C **83-293** (2023) https://doi.org/10.1140/epjc/s10052-023-11353-w
8. M. Abbrescia et al., Observation of Rayleigh-Lamb waves generated by the 2022 Hunga-Tonga volcanic eruption with the POLA detectors at ny-Ålesund. Sci. Rep. **12** (2022) https://doi.org/10.1038/s41598-022-23984-2
9. R.R.S. deMendonça et al., Temperature effect in secondary cosmic rays (muons) observed at the ground: analysis of the global muon detector network data. The Astrophysical Journal **830**(2) (2016) https://doi.org/10.3847/0004-637X/830/2/88
10. J.T. VanderPlas, Understanding the lomb–scargle periodogram. Astrophys. J. Suppl. Ser. **236**(1), 16 (2018). https://doi.org/10.3847/1538-4365/aab766
11. GMDN: Global Muon Detector Network Data. http://hdl.handle.net/10091/0002001448 Accessed 2025-07-23
12. C.A.O.S. Zhang JiLong, Institute of High Energy Physics: YBJ International Cosmic Ray Observatory. http://ybjnm.ihep.ac.cn/mu/ Accessed 2025-07-22
13. C. Katoa et al., New cosmic ray observations at Syowa station in the antarctic for space weather study. J. Space Weather Space Clim. **11**, 31 (2021)
14. T.Gaisser et al., Seasonal variation of atmospheric muons in Icecube. Proceedings of Science (2021) https://doi.org/10.22323/1.358.0894
15. N.Y. Agafonova et al., Exploration of the stratosphere with cosmic-ray muons detected underground. Phys. Rev. Res. **4**, 023226 (2022). https://doi.org/10.1103/PhysRevResearch.4.023226
16. NMDB: Neutron Monitor Database. https://www.nmdb.eu/nest/search.php Accessed 2025-07-22
17. J. Jeong, S. Oh, Seasonal trends of the cosmic ray intensity observed by 16 neutron monitors for 1964–2020. Adv. Space Res. **70**(9), 2625–2635 (2022). https://doi.org/10.1016/j.asr.2022.02.052